Evaluation of internal rotation gait and normal gait based on the interarticular coordination

Natsuki Sai, Tatsuro Sato, Shinichiro Morichi, Satoru Kizawa, and Ayuko Saito

Department of Mechanical Science and Engineering, School of Advanced Engineering, Kogakuin University, Tokyo, Japan
E-mail: s519022@ns.kogakuin.ac.jp

Abstract
This study investigates the coordination between the joint angles of lower limbs during normal gait and internal rotation gait by applying singular value decomposition. The results indicated that the ankle abduction, the ankle internal rotation, the hip flexion were generated during internal rotation gait.

The symptoms of the disorder in central nervous system patients such as cerebral palsy change due to growth [1]. The tests for cerebral palsy include imaging of the brain, such as ultrasound, CT scan, or MRI. These tests help to distinguishing between cerebral palsy and other possible causes. Sedatives may be used to keep body stationary during those tests. However, sedative use may lead to side effects for children [2]. On the hand, motion analysis can be used to detect abnormal gait caused by central nervous disorder. The optical motion capture system used for motion analysis requires many markers to be attached to the body. Moreover, distinguishing internal rotation gait from spastic gait caused by central nervous system disorder is not easy. Detecting gait characteristic of children with spastic cerebral palsy by simple motion analysis enables to find disease in the early-stage such as regular checkups for infants. Therefore, in this research, as a first step to build a method of identifying internal rotation gait and spastic gait, we attempt to detect the characteristics of normal gait and internal rotation gait of healthy people. This study investigates the coordination between the joint angles of lower limbs during normal gait and internal rotation gait by applying singular value decomposition. The dominant coordination pattern is obtained by applying singular value decomposition on the joint angles of lower limbs measured during the experiment [3].

Healthy participant is examined during the experiment. Following an explanation of the purpose and requirements of the study, the participants gave their written informed consent to participate. Study approval was obtained from the Research Ethics Board, Kogakuin University, and the National Institute of Technology, Akita College.

During the experiment kinematic and kinetic data were collected simultaneously using an optical motion capture system (Bonita 10; Vicon Motion Systems, Ltd.) and two force plates (9286; Kistler Japan Co., Ltd.). The two force plates were placed on the walking path shown in Fig. 1. During the experiment, the participant stepped with their left foot on the first force plate and their right on the second. The sampling frequencies of the optical motion capture system and the force plates were 100 Hz.

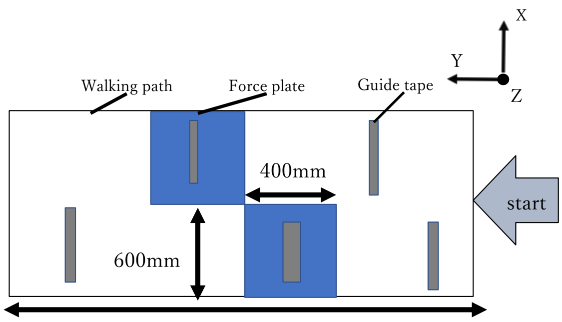

Fig.1 Walking path.

The positions of the reflective markers for the optical motion capture system were set in accordance with the Plug-in Gait lower body marker set.

Markers were placed at the heel contact point on the walking path based on each participant's natural stride length. The participants were instructed to walk using a natural stride in time with a metronome (110 bpm). They performed the task with a normal gait and a internal rotation gait three times each. After the experiment, markers were labeled using analysis software (Nexus2, manufactured by Vicon). Knee joint angles were obtained by running the Plug-in Gait Dynamic pipeline.

The joint angles of the participant are depicted in Figs. 2 to 4. Black solid curves represent the average values of five trials during normal gait. Red solid curves represent the average values of five trials during internal rotation gait. The dashed curves represent the standard deviations of five trials. The walking cycle is 100%, which extends from the beginning of the stance phase until the end of the swing phase. Figure 2 represents that the ankle joint angle during internal rotation gait was much more abduction and internally rotated than the result during normal gait. Figure 3 represents that there was no clear difference in flexion and extension of the knee joint. Figure 4 represents that the hip joint angle during internal rotation gait was much more adducted and internally rotated than the result during normal gait. The results indicate that there are clear differences in

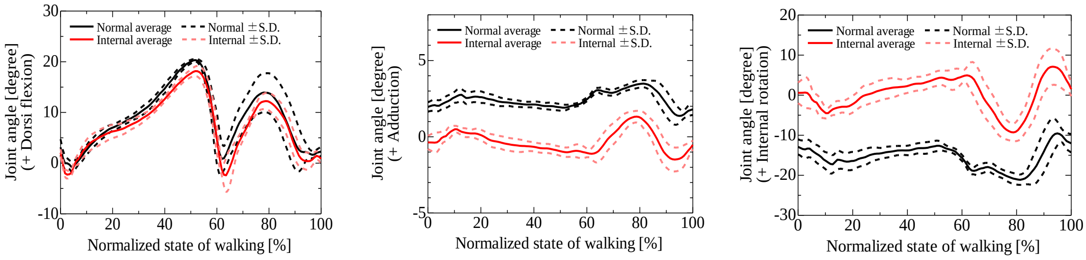

(a) Dorsi - plantar flexion *(b) Adduction - abduction* *(c) Internal - external rotation*

Fig. 2 Left ankle joint angle obtained from 3D motion capture system.

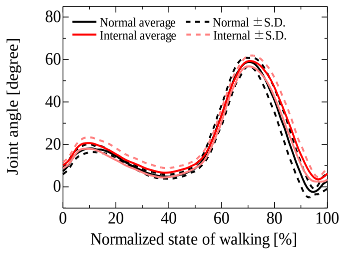

Fig.3 Left knee joint angle obtained from 3D motion capture system (Flexion - extension).

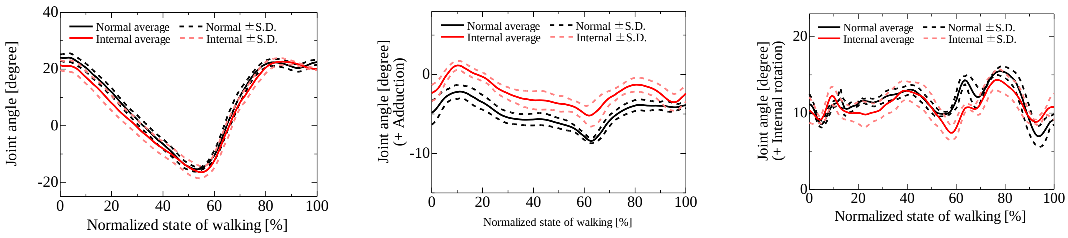

(a) Flexion - extension *(b) Adduction - abduction* *(c) Internal - external rotation*

Fig. 4 Left hip joint angle obtained from 3D motion capture system.

the results between normal gait and internal rotation gait of a healthy subject.

The coordination between the lower limbs of a person walking normally and internal rotationally was examined by applying singular value decomposition.

Lower limb joint angles were converted into dimensionless quantities of -1 to 1 as follows:

$$\theta(t) = \frac{2(\theta_{raw}-\theta_{min})}{\theta_{max}-\theta_{min}} - 1 \qquad (1)$$

where θraw (t) represents the joint angles obtained from an optical 3D motion capture system; θmax, and θ min respectively represent the maximum, and minimum joint angles for each joint.

The observation matrix consists of dimensionless quantities of lower limb joint angles. The observation matrix R(θ, t) is composed in Fig.2.

Where θ_{Lxank}, θ_{Lyank}, θ_{Lzank}, θ_{Rxank}, θ_{Ryank} and θ_{Rzank} respectively represent the angles of drosal, abduction, and internal rotation in the left and right ankle; θ_{Lxkne} and θ_{Rxkne} respectively represent the angles of flexion in the left and right knee; θ_{Lxhip}, θ_{Lyhip}, θ_{Lzhip}, θ_{Rxhip}, θ_{Ryhip} and θ_{Rzhip} respectively represent the angles of flexion, abduction, and internal rotation in the left and right hip; and *m* represents the number of time-series data points.

The observation matrix [Eq. (2)] is decomposed into the basis vectors as

$$(\theta, t) = \begin{pmatrix} \theta_{Lxank}(t_1) & \theta_{Lyank}(t_1) & \theta_{Lzank}(t_1) & \theta_{Lxhip}(t_1) & \theta_{Lyhip}(t_1) & \theta_{Lyhip}(t_1) & \theta_{Lzhip}(t_1) & \theta_{Rxank}(t_1) & \cdots & \theta_{Rzhip}(t_1) \\ \vdots & \vdots & \vdots & \vdots & \vdots & \vdots & \vdots & \vdots & \vdots & \vdots \\ \theta_{Lxank}(t_m) & \theta_{Lyank}(t_m) & \theta_{Lzank}(t_m) & \theta_{Lxhip}(t_m) & \theta_{Lyhip}(t_m) & \theta_{Lyhip}(t_m) & \theta_{Lzhip}(t_m) & \theta_{Rxank}(t_m) & \cdots & \theta_{Rzhip}(t_m) \end{pmatrix} \qquad (2)$$

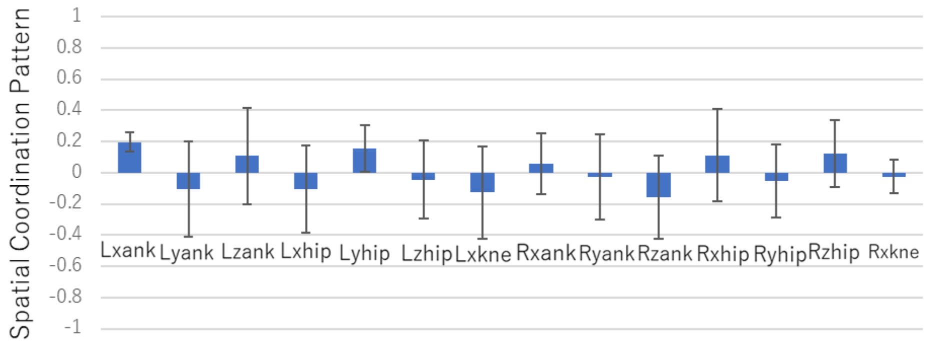

Fig. 5 Spatial coordination pattern of the fist mode of the normal gait..

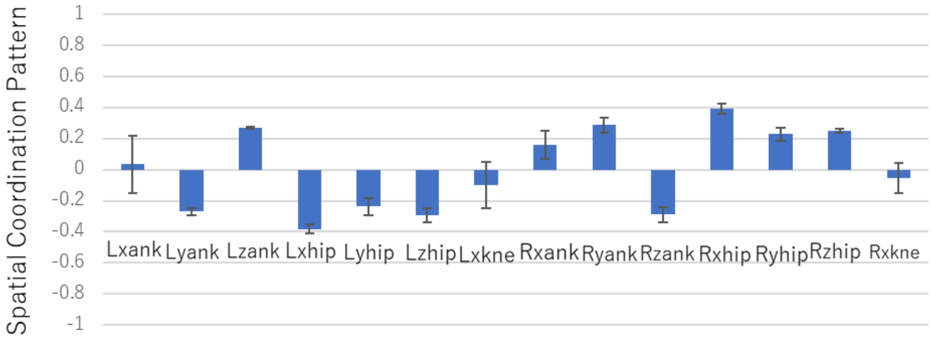

Fig.6 Spatial coordination pattern of the fist mode of the internal rotation gait..

$$R(\theta,t) = \sum_{i=1}^{n} \lambda_i V_i\,(t) Z_i^{\ T}(\theta) \qquad (3)$$
$$(\ i = 1, \dots, n, \quad n = 14)$$

where λ_i is a singular value; Z_i is a dominant coordination pattern. The motion modes are defined in descending order of λ_i.

The contribution ratioγ_i of the singular value in the i-th motion mode is

$$\gamma_i = \frac{\lambda_i}{\sum_{i=1}^{n} \lambda_i^{\ 2}} \quad (\ i = 1, \dots, n, \quad n = 14) \qquad (4)$$

where i is the number of columns in the observation matrix.

The contribution ratio of the first mode was calculated to be about 34~54%. Consequently, we concluded that the first mode was the dominant motion mode in each trial. The spatial basis results, which represent the coordination patterns, are shown in Figs. 5 and 6. Figure 5 is the result of the normal gait. Figure 6 is the result of the internal rotation gait. In the case of the normal gait, there was no significant change in the value difference. However, in the internal rotation gait result, the abduction angle of the ankle, the internal rotation angle of the ankle, the flexion angle of the hip joint, the abduction angle, and the internal rotation angle were generated. As a result, we concluded that those results were coordination patterns during normal gait and internal rotation gait.

References:

[1] M. Nakajima et al., Developmental changes in the Collis horizontal reaction analyzed using a three-dimensional video motion analysis system. I. Examination of techniques for inducing Collis horizontal reaction, Japanese society of child neurology, Vol. 37, No. 6 (2005), pp. 479-485 (in Japanese).

[2] E. Suzuki et al., Evaluation on spastic gait caused by cervical myelopathy with gait analysis, Proceedings of annual meeting of Japanese society for clinical biomechanics and related research, Vol. 23(2002), pp. 447-451 (in Japanese).

[3] T. Funato et al., Quantitative evaluation of the intersegmental coordination during human locomotion, Journal of the Robotics Society of Japan, Vol. 28, No. 8 (2010), pp. 996-1003 (in Japanese).